

## Radiative lifetimes and transition probabilities for electric-dipole $\Delta n = 0$ transitions in highly stripped sulfur ions\*

D. J. Pegg, S. B. Elston, P. M. Griffin, H. C. Hayden,<sup>†</sup> J. P. Forester, R. S. Thoe, R. S. Peterson, and I. A. Sellin

*University of Tennessee, Department of Physics, Knoxville, Tennessee 37916  
and Oak Ridge National Laboratory, Oak Ridge, Tennessee 37830*

(Received 27 May 1976)

The beam-foil time-of-flight method has been used to investigate radiative lifetimes and transition rates involving  $\Delta n = 0$  allowed transitions within the  $L$  shell of highly ionized sulfur. The results for these transitions, which can be particularly correlation sensitive, are compared to current calculations based upon multiconfigurational models.

### INTRODUCTION

Transition probabilities or, equivalently, absorption oscillator strengths ( $f$  values) for atoms and ions are fundamentally important atomic quantities which find frequent practical application in many areas of research, e.g., astrophysics, laser physics, and plasma physics. For example, there exists an urgent need at the present time for  $f$  values of resonance transitions of high- $Z$  heavy ions which form impurities in magnetically confined thermonuclear plasmas.<sup>1</sup> These impurities, although only believed to be present in small concentrations, are thought to contribute strongly to radiative energy losses from the plasma.

Recent studies<sup>2</sup> of the systematic trends of dipole ( $E1$ )  $f$  values along isoelectronic sequences, which are based upon the nonrelativistic perturbation expansion of  $f$  values in terms of the inverse nuclear charge, have proven to be extremely valuable for low-to-intermediate- $Z$  ions. Beam-foil results in this region have been very instrumental in the establishment of such trends along many sequences including the detection of certain  $f$ -value anomalies brought about by configurational level crossings or cancellations of transition integrands. It is in this region of low to intermediate  $Z$  that electron correlation effects can become important particularly for transitions in which the principal quantum number of the active electron does not change in the transition, i.e.,  $\Delta n = 0$  (intrashell) transitions. These intrashell or "shell-equivalent" transitions are particularly correlation sensitive owing to the interpenetration of the electrons of the same principal quantum number, and many-particle atomic models which include configuration mixing effects are used to replace the simple independent-particle picture. Correlation effects, although usually most important for low- $Z$  ions, are not entirely negligible for such intermediate- $Z$  ions as sulfur, which is being studied here. For some transitions, how-

ever, limited mixing with adjacent configurations of the same shell is found to be sufficient but this may not be the case for other transitions studied. The present work on  $\Delta n = 0$  transitions within the  $L$  shell of sulfur ions represents a considerable extrapolation in nuclear charge along the isoelectronic sequences of all the transitions studied. Results for even higher- $Z$  ions will be necessary in order that one may confidently extrapolate the existing nonrelativistic systematic curves into the very-high- $Z$  region where relativistic effects on  $f$  values, such as orbital shrinkage and configurational effects involving the breakdown of the  $LS$  coupling scheme, become appreciable. Recent relativistic  $f$ -value calculations by Kim and Desclaux,<sup>3</sup> Weiss,<sup>4</sup> and Lin and Armstrong<sup>5</sup> indicate that in the cases of the Li and Be sequence, for example, the calculated  $f$  value for the resonance lines begins to depart significantly from the nonrelativistic value around  $Z \sim 25$ . A selected number of experimental beam-foil results in this uncharted relativistic regime could greatly serve to guide theoretical progress.

Comparisons of accurately measured electric dipole transition probabilities or  $f$  values with calculations of such quantities afford sensitive tests of the correctness of the wave functions in the upper and lower states of the transition. Two distinct types of allowed radiative processes can be distinguished. "Out-of-shell," intershell or  $\Delta n \neq 0$  transitions, whose rates scale as  $Z^4$  along an isoelectronic sequence and "in-shell," intrashell or  $\Delta n = 0$  transitions, which scale linearly with  $Z$ . The  $\Delta n \neq 0$  transitions become too rapid for the beam-foil time-of-flight method for large- $Z$  low- $N$  ions ( $N$  is the number of electrons) but  $\Delta n = 0$  transitions remain accessible to beam-foil studies to surprisingly high  $Z$  owing, of course, to the considerably weaker  $Z$ -scaling dependence. It is these  $\Delta n = 0$  transitions of the type  $2s^2 2p^n - 2s 2p^{n+1}$  and  $2p^n - 2p^{n+1}$ , within the  $L$  shell of sulfur, that are studied in the present work. Figure 1

shows a partial energy-level diagram of the  $n=2$  manifold of states associated with the carbonlike ion  $S^{10+}$  to illustrate this type of transition.

Such  $\Delta n=0$  transitions are particularly important since they constitute, for example, the strong resonance lines of atoms and ions of the first and second rows of the Periodic Table. Many of the transitions studied in the present work are also prominent in the solar spectrum<sup>6</sup> and thus could find practical application in sulfur-abundance determinations, for example.

#### EXPERIMENTAL METHOD

The Oak Ridge National Laboratory tandem accelerator was used to obtain a magnetically analyzed 38-MeV sulfur-ion beam. The beam was collimated and sent through a thin carbon foil ( $\sim 5 \mu\text{g}/\text{cm}^2$  thickness) which served to both further strip and excite the beam ions. In this method, the beam-foil-excitation technique, the post-foil beam emerges in a distribution of charge states whose mean is determined by the incident beam energy. The charge state distribution for 38-MeV sulfur ions incident on a thin carbon foil is shown, as given by Wittkower and Betz,<sup>7</sup> in Fig. 2. Extreme ultraviolet (EUV) radiation emitted in flight by the decaying foil-excited ions was collected

perpendicular to the beam direction and dispersed with the 2.2-m grazing-incidence spectrometer shown schematically in Fig. 3. The gold-coated (300 grooves/mm) concave grating used in the instrument has a blaze angle of  $2^\circ 4'$  (blaze wavelength of  $191 \text{ \AA}$  at an angle of incidence of  $87.5^\circ$ ). A hollow cathode discharge source, which is not shown in the figure, is situated directly opposite the entrance slit of the spectrometer. This source can be used to periodically calibrate the instrument during a run using, for example, the well-established resonance lines of He and  $\text{He}^+$ . A low-noise ( $\sim 0.08 \text{ Hz}$ ) electron channel multiplier (channeltron) is positioned behind the exit slits of the spectrometer and a 90% transmission grid is used to bias out stray electrons. The spectrometer could be stepped in discrete and variable wavelength intervals and the detector output, which was normalized to a fixed amount of beam charge collected in a well-shielded Faraday cup, could be stored in a multichannel scaler that was synchronized with the stepping process. Examples of EUV spectra, taken at a fixed distance behind the foil, are shown in Figs. 4 and 5. The linewidths [full width at half-maximum (FWHM)] in these spectra, mostly instrumental in origin, are  $0.75 \text{ \AA}$ . Doppler broadening of the lines due to the finite

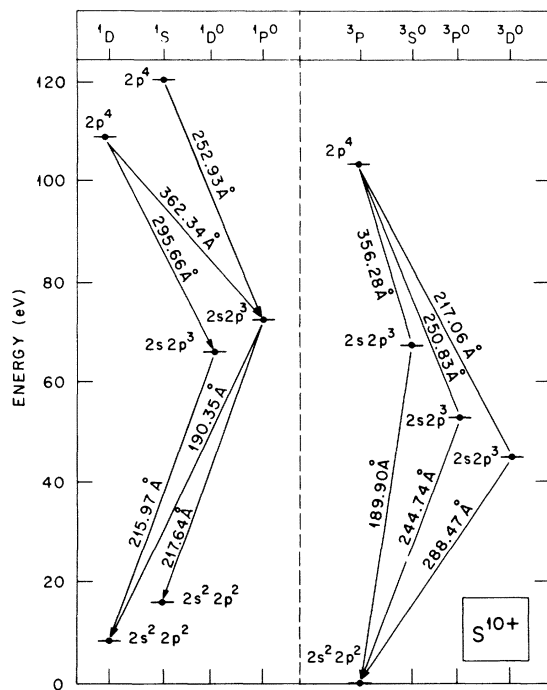
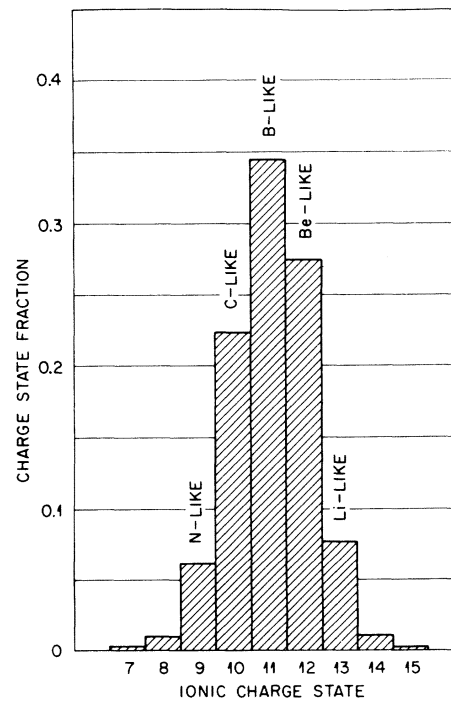


FIG. 1. Partial energy-level diagram showing  $\Delta n=0$  transition within the  $n=2$  manifold of states in the carbonlike ion  $S^{10+}$ . The wavelengths shown are multiplet averages derived from Ref. 8.



38-MeV Sulfur on Carbon Foil.

FIG. 2. Post-foil charge state distributions following the transmission of a 38-MeV sulfur-ion beam through a thin carbon foil.

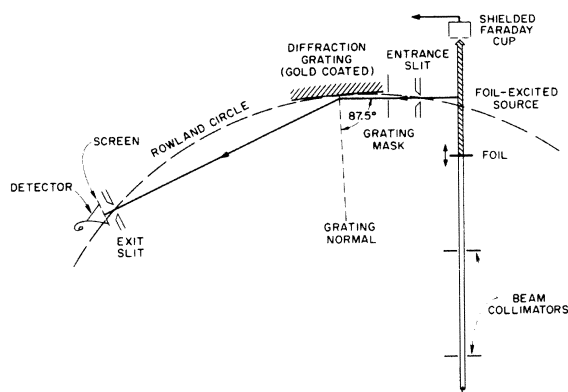


FIG. 3. Schematic diagram of the essential experimental arrangement used in the present work (not to scale).

but small entrance aperture was negligible in this spectral region. The spatial resolution along the beam, which is determined by the beam-spectrometer geometries, was  $300\ \mu\text{m}$  in this experimental arrangement. This corresponds to a temporal resolution of  $\sim 20$  psec for a 38-MeV sulfur-ion beam.

Time-of-flight lifetime measurements were made on the most intense and unblended features by observing (photoelectrically) the intensity of a wavelength-selected line as a function of the spatial distance between the point of initial excitation, i.e., the back surface of the foil, and the viewing region of the spectrometer. The spatial decay can be converted to a temporal decay via the constant velocity of the beam. For transitions involving unity branching ratios, such lifetime measurements can be used to obtain the fundamentally important quantities, atomic transition probabili-

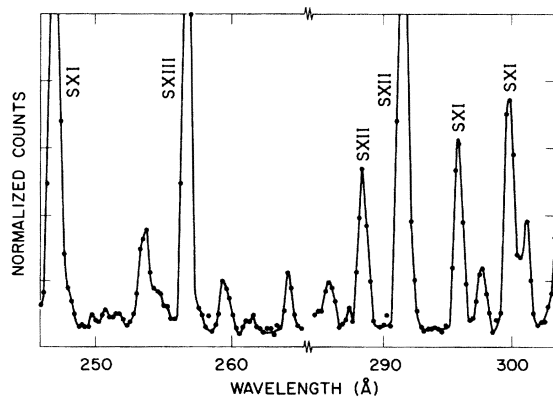


FIG. 4. Portion of an EUV spectral scan of the foil-excited sulfur source from  $\sim 250$ – $300\ \text{\AA}$ . The incident beam energy is 38 MeV. The charge states of the most prominent features are shown. The linewidth of  $\sim 0.75\ \text{\AA}$  (FWHM) is almost entirely instrumental.

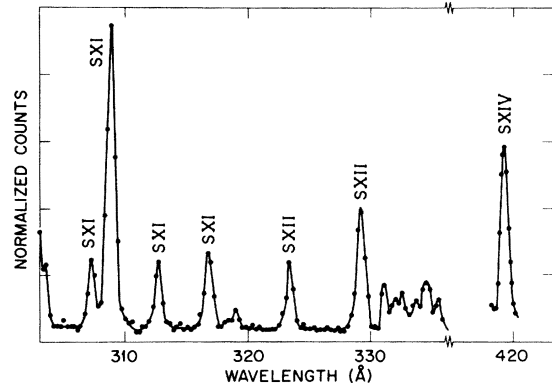


FIG. 5. Same as in Fig. 4 except wavelength interval from  $300$ – $420\ \text{\AA}$ .

ties ( $A_{ij}$ ) or, equivalently, the multiplet oscillator strengths ( $f_{ji}$ ), via the well-known relationships

$$A_{ij} = 1/\tau_i$$

and

$$f_{ji} = 1.4992 \times 10^{-16} \bar{\lambda}_{ij}^2 (g_i/g_j) (1/\tau_i),$$

where  $\tau_i$  is the lifetime of the upper state (sec),  $g_i, g_j$  are the statistical weights of the upper and lower states, respectively, and  $\bar{\lambda}_{ij}$  is the average

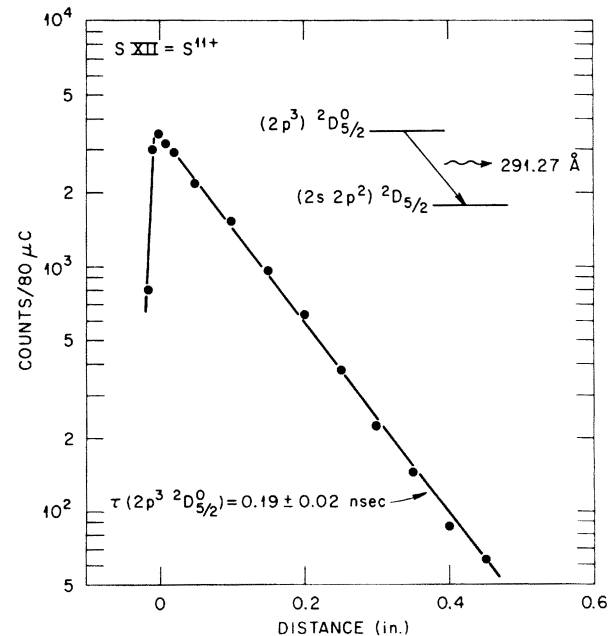


FIG. 6. Typical time-of-flight decay curve for an allowed  $\Delta n = 0$  transition in boronlike sulfur. The  $x = 0$  or foil surface position occurs at the intensity maximum. The spatial distance of  $0.2$  in. corresponds to a temporal delay of  $336$  psec using a 38-MeV sulfur beam. The semilog plot of this decay is seen to be linear over more than three decay lengths.

multiplet wavelength of the transition, which was derived using the recent tabulation of Fawcett.<sup>8</sup> The present results are estimated to be uncertain to  $\sim \pm 10\%$ . Typical time-of-flight decay curves are shown in Figs. 6–8. In all cases possible the intensity decay was studied to at least three decay lengths in order to look for long-lived decay components brought about by cascading and/or line blending within the instrumental bandpass. In most of the work studied here no long-lived components were observed in the decay curves, which is to be expected since the upper states involved in these allowed intrashell transitions themselves are the longest-lived excited states of the ion. “Out-of-shell” cascade transitions, whose rates scale as a factor of  $Z^3$  faster than the “in-shell” rates, are expected to “dump” their population very close to the foil. We were very careful in defining the point of excitation, i.e.,  $x=0$ , in these studies in order to try to observe very-short-lived cascade components but again, in most cases, cascading is not found to be a problem. Cascades, when present, are in-shell processes. Figure 6 indicates

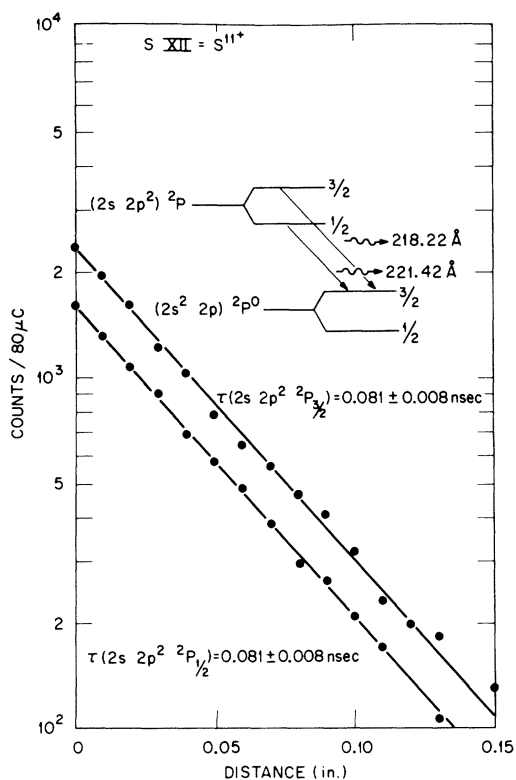


FIG. 7. Spatial decay-in-flight curves for resonance transitions in the boronlike sulfur ion,  $S^{11+}$ . The upper and lower decay curves represent the decay of the  $J = \frac{3}{2}$  and  $J = \frac{1}{2}$  levels, respectively. The semilog plots of the decays are both linear over more than three decay lengths.

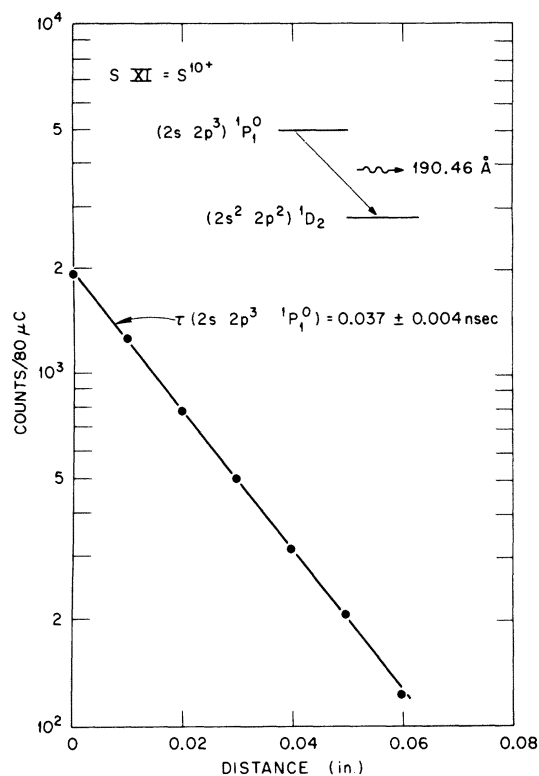


FIG. 8. Spatial decay-in-flight curve for the transition indicated in carbonlike sulfur,  $S^{10+}$ . The semilog plot of the decay is seen to be linear for  $\sim 100$  psec which is equivalent to approximately three decay lengths.

how the  $x=0$  position is defined by translating the foil slowly into the viewing region and recording the initial build-up in intensity to a maximum. This maximum corresponds to the viewing region being completely filled by the foil-excited beam source. In the other decay curves of Figs. 7 and 8 the intensity decay is shown starting from the measured  $x=0$  position.

## RESULTS

Tables I and II show the measured lifetimes and transition rates, respectively, along with some theoretical results. The calculations of Safronova *et al.*<sup>9</sup> and Cohen and Dalgarno<sup>10</sup> are both based upon the nuclear-charge expansion perturbation method which includes only limited configuration interaction. For intermediate- $Z$  ions such as sulfur, however, there appears little difference for most transitions between the results of Safronova *et al.*<sup>9</sup> and those of Sinanoğlu.<sup>11</sup> The latter results represent a more sophisticated electron correlation treatment (the results for sulfur ions are derived from a linear extrapolation of the  $f$  value that is quoted by Sinanoğlu<sup>11</sup> for isoelec-

TABLE I. Lifetimes in highly ionized sulfur.

Number of electrons	Wavelength (Å)	Upper level	Lifetimes ( $10^{-12}$ sec)	
			Present <sup>a</sup>	Theory <sup>b</sup>
4	256.70	$(2s, 2p)^1P^o_1$	160	135, <sup>c</sup> 129 <sup>d</sup>
4	308.95	$(2p^3)^3P_2$	168	168, <sup>c</sup> 156 <sup>d</sup>
5	288.39, 299.64	$(2s2p^2)^2D_{3/2,5/2}$	410	383, <sup>c</sup> 344, <sup>d</sup> 385 <sup>e</sup>
5	291.27	$(2p^3)^2D_{5/2}$	190	146 <sup>c</sup>
5	218.23, 221.44	$(2s2p^2)^2P_{3/2,1/2}$	81	50, <sup>c</sup> 46, <sup>d</sup> 48 <sup>e</sup>
5	243.00	$(2p^3)^4S_{3/2}$	90	54, <sup>c</sup> 49 <sup>d</sup>
6	190.46	$(2s2p^3)^1P^o_1$	39	29, <sup>c</sup> 32 <sup>e</sup>
6	216.00	$(2s2p^3)^1D^o_2$	73	47, <sup>c</sup> 41, <sup>d</sup> 77 <sup>e</sup>
6	188.69	$(2s2p^3)^3S^o_1$	35	23, <sup>c</sup> 21, <sup>d</sup> 22 <sup>e</sup>
6	247.10	$(2s2p^3)^3P^o_1$	150	136, <sup>c</sup> 114, <sup>d</sup> 133 <sup>e</sup>
6	295.59	$(2p^4)^1D_2$	70	72, <sup>c</sup> 67 <sup>d</sup>
7	180.77	$(2s2p^4)^2P_{3/2}$	23	20, <sup>c</sup> 19 <sup>e</sup>

<sup>a</sup> Estimated uncertainty,  $\pm 10\%$ .

<sup>b</sup> Average wavelengths used in conversion from Ref. 8.

<sup>c</sup> Reference 9.

<sup>d</sup> Reference 10.

<sup>e</sup> Reference 11.

tronic silicon ions). It can be seen from the tables that, in general, the measured lifetimes are longer than predicted by current theory by up to 40%. Of course, transition probabilities, where derivable, are lower than corresponding theoretical predictions by the same amount. Since cascading and/or blending do not in general appear to be a major problem in the present experiments, it is suspected that insufficient mixing effects have been taken into account in the multiconfigurational calculations. In cases such as the  $(2s2p)^3P^o - (2p^2)^3P$  transition in the Be sequence ( $S^{12+}$ ), where configuration mixing is expected to be very small, there exists excellent agreement between theory and the present result. In contrast, however, the

measured transition probability for the  $(2s^22p)^2P^o - (2s2p^2)^2P$  transition in the B sequence ( $S^{11+}$ ) is found to be  $\sim 40\%$  lower than the current theoretical values. In addition, this difference between theory and beam-foil measurements appears to continue, by roughly the same amount, to lower- $Z$  members of the sequence for this particular transition. Strong mixing effects between the ground-state  $2s^22p^n$  and the excited-state configurations  $2p^{n+2}$  (same parity and within the same shell) will occur, particularly for the low- $Z$  end of the sequences. Mixings between  $L$ -shell configurations and higher-shell configurations are expected to be small especially for intermediate- $Z$  ions such as sulfur.

TABLE II. Transition probabilities for some allowed  $\Delta n = 0$  transitions of highly ionized sulfur.

Number of electrons	Transition	Transition probability ( $10^9$ sec <sup>-1</sup> )	
		Present <sup>a</sup>	Theory <sup>b</sup>
4	$(2s^2)^1S - (2s2p)^1P^o$	6.25	7.42, <sup>c</sup> 7.77 <sup>d</sup>
4	$(2s2p)^3P^o - (2p^2)^3P$	5.95	5.96, <sup>c</sup> 6.40 <sup>d</sup>
5	$(2s^22p)^2P^o - (2s2p^2)^2D$	2.44	2.61, <sup>c</sup> 2.90, <sup>d</sup> 2.60 <sup>e</sup>
5	$(2s^22p)^2P^o - (2s2p^2)^2P$	12.35	19.80, <sup>c</sup> 21.65, <sup>d</sup> 20.79 <sup>e</sup>
5	$(2s2p^2)^4P - (2p^3)^4S^o$	11.11	18.45, <sup>c</sup> 20.35 <sup>d</sup>
6	$(2s^22p^2)^1D - (2s2p^3)^1D^o$	13.70	21.45, <sup>c</sup> 24.64, <sup>d</sup> 13.01 <sup>e</sup>
6	$(2s^22p^2)^3P - (2s2p^3)^3S^o$	28.57	44.39, <sup>c</sup> 47.79, <sup>d</sup> 45.21 <sup>c</sup>
6	$(2s^22p^2)^3P - (2s2p^3)^3P^o$	6.67	7.35, <sup>c</sup> 8.74, <sup>d</sup> 7.51 <sup>e</sup>

<sup>a</sup> Estimated uncertainty,  $\pm 10\%$ .

<sup>b</sup> Average wavelengths used in conversion from Ref. 8.

<sup>c</sup> Reference 9.

<sup>d</sup> Reference 10.

<sup>e</sup> Reference 11.

\*Research supported in part by the National Science Foundation, by the Office of Naval Research, by the National Aeronautics and Space Administration, and by Union Carbide Corporation under contract with the U. S. Energy Research and Development Agency.

†Permanent address: Dept. of Physics, Univ. of Connecticut, Storrs, Conn. 06268.

<sup>1</sup>E. Hinnov, Princeton University Report No. MATT-1022, 1974 (unpublished).

<sup>2</sup>W. L. Wiese and A. W. Weiss, Phys. Rev. 175, 50 (1968); M. W. Smith and W. L. Wiese, Astrophys. J. Suppl. No. 196, 23, 103 (1971).

<sup>3</sup>Y. K. Kim and J. P. Desclaux, Phys. Rev. Lett. 36, 139 (1976).

<sup>4</sup>A. W. Weiss, in *Beam-Foil Spectroscopy*, edited by

I. A. Sellin and D. J. Pegg (Plenum, New York, 1976), Vol. I.

<sup>5</sup>D. L. Lin and L. Armstrong, Jr., Bull. Am. Phys. Soc. 21, 626 (1976).

<sup>6</sup>M. Malinovsky and L. Heroux, Astrophys. J. 181, 1009 (1973).

<sup>7</sup>A. B. Wittkower and H. D. Betz, At. Data Tables 5, 113 (1973).

<sup>8</sup>B. C. Fawcett, At. Data Nucl. Data Tables 16, 135 (1975).

<sup>9</sup>U. I. Safronova, A. N. Iranova, and V. N. Kharitonova, Theor. Exp. Chem. (USSR) 5, 209 (1969).

<sup>10</sup>M. Cohen and A. Dalgarno, Proc. R. Soc. A 280, 258 (1964).

<sup>11</sup>O. Sinanoğlu, Nucl. Instrum. Methods 110, 193 (1973).